·临床研究·

主动脉瓣狭窄对升主动脉瘤流场特征的影响

李昊天[1]，吕　磊[1]，杨淞然[2]，华　平[1]
(1. 中山大学孙逸仙纪念医院心血管外科，广东 广州 510120；2. 中山大学孙逸仙纪念医院生物治疗中心，广东 广州 510120)

摘　要：【目的】基于计算流体力学技术，及血流动力学指标评价主动脉瓣狭窄对升主动脉瘤流场特征的影响。【方法】回顾性分析2017年1月至2021年12月中山大学孙逸仙纪念医院63名升主动脉扩张或升主动脉瘤的入院患者，根据瓣口面积分为主动脉瓣狭窄组及非狭窄组，对两组患者进行倾向性匹配分析后，比较两组的血流动力学指标(如：压力、剪切应变率(SSR)、壁面剪切力(WSS)、时间均化剪切应变率(TASSR)和时间均化壁面剪切力(TAWSS))；并根据中心线划分升主动脉为6块具有独特空间特征的区域，比较两组6块区域之间血流动力学指标的差异。【结果】主动脉瓣狭窄组升主动脉的SSR(191.70 [117.22~248.78] s^{-1})和WSS(2.87 [1.88~4.00] Pa)与非狭窄组的SSR(93.23 [68.59~145.35] s^{-1})和WSS(1.20 [1.04~2.18] Pa)相比，差异具有统计学意义(SSR：$Z = 2.167$，$P = 0.030$；WSS：$Z = 2.233$，$P = 0.026$)，且差异主要表现在升主动脉近端及小弯侧($P < 0.05$)。而压力、TASSR或TAWSS的差异无统计学意义。【结论】主动脉瓣狭窄改变了升主动脉扩张或升主动脉瘤的血流动力学，增大了正切于血管的力(如：SSR、WSS)，而对垂直于血管的力(如：压力)无明显的影响。

关键词：主动脉瓣狭窄；升主动脉瘤；流体力学；血流动力学指标；倾向性评分匹配
中图分类号：R654.3　　**文献标志码**：A　　**文章编号**：1672-3554(2022)03-0462-09
DOI：10.13471/j.cnki.j.sun.yat-sen.univ(med.sci).2022.0314

Effects of Aortic Valve Stenosis on the Flow Field Characteristics of Ascending Aortic Aneurysm

LI Hao-tian[1], LÜ Lei[1], YANG Song-ran[2], HUA Ping[1]
(1. Department of Cardiovascular Surgery, Sun Yat-sen Memorial Hospital, Sun Yat-sen University, Guangzhou 510120, China; 2. Department of Biotherapy Center, Sun Yat-sen Memorial Hospital, Sun Yat-sen University, Guangzhou 510120, China)
Correspondence to: HUA Ping, E-mail: huaping@mail.sysu.edu.cn; YANG Song-ran, E-mail: yangsr@mail.sysu.edu.cn

Abstract:【Objection】To evaluate the effects of aortic valve stenosis on the flow field characteristics of ascending aortic aneurysm by computational fluid dynamics and hemodynamic indexes.【Methods】A total of 63 patients aged 18 or over with ascending aortic dilation or aneurysm were retrospectively recruited from Sun Yat-sen Memorial Hospital of Sun Yat-sen University and assigned to aortic valve stenosis (AS) or none aortic valve stenosis (NAS) group. Propensity score matching analysis and ascending aortic division based on centerline were performed to compare the hemodynamic indexes [pressure, shear stress rate (SSR), wall shear stress (WSS), time average shear stress rate (TASSR), time average wall shear stress (TAWSS)].【Results】There were significant differences in SSR (191.70 [117.22~248.78] s^{-1} *vs.* 93.23 [68.59~145.35] s^{-1}, $Z = 2.167$, $P = 0.030$) and WSS (2.87 [1.88~4.00] Pa *vs.* 1.20 [1.04~2.18] Pa, $Z = 2.233$, $P =$

收稿日期：2022-02-25
基金项目：国家自然科学基金(81771165)；广东省自然科学基金(2020A1515010233，2018A030313172)；广州市科技计划项目(201704030032；201807010010)
作者简介：李昊天，研究生，研究方向：心血管外科，E-mail：a793062387@gmail.com；华平，通信作者，教授，研究方向：心血管外科，E-mail：huaping@mail.sysu.edu.cn；杨淞然，通信作者，教授，研究方向：心血管外科，E-mail：yangsr@mail.sysu.edu.cn

0.026) between AS group and NAS group. The differences were mainly found in the proximal and lesser curvature of ascending aorta ($P < 0.05$). There was no statistical significance in pressure, TASSR or TAWSS.【Conclusions】Aortic valve stenosis alters the hemodynamics in ascending aortic dilation or aneurysms, which increases tangential component force (e.g. SSR, WSS) but has no significant effects on perpendicular component force (e.g. pressure).

Key words: aortic valve stenosis; ascending aortic aneurysm; computational fluid dynamics; hemodynamic index; propensity score matching

[J SUN Yat-sen Univ(Med Sci), 2022, 43(3): 462-470]

主动脉瓣狭窄是一种常见的心脏畸形，多由老年性主动脉钙化、风湿性心脏病和先天性畸形导致，同时也是升主动脉扩张、升主动脉瘤及血管破裂的危险因素[1]。有证据表明，升主动脉扩张乃至成瘤常与主动脉瓣的改变高度相关[2]，但是其流场特征的变化却不甚明了。如今，流场特征在评估大动脉疾病风险的重要价值逐渐被发现，例如，在主动脉中壁面剪切力升高常引起血管扩张，而低的壁面剪切力在动脉粥样硬化斑块形成中起到调控血管内皮细胞病理生理的作用[3]。此外，多种多样的血流动力学指标，如：压力，剪切应变率及时间均化的壁面剪切力[4-5]等，都在认识主动脉疾病中发挥新的作用[6]。然而临床上通过仪器直接测量大血管的血流动力学指标常面临着有创、精度低及人力成本高等缺点，这些缺点随着计算机技术的发展，被流体力学技术所解决[7-8]。本研究中，我们基于流体力学软件及有限元分析精确、快速地计算出伴有主动脉瓣狭窄或非狭窄的升主动脉瘤的5种血流动力学指标[压力，剪切应变率（shear stress rate, SSR），壁面剪切应力（wall shear stress, WSS），时均剪切应变率（time average shear stress rate, TASSR），时均壁面剪切应力（time average wall shear stress, TAWSS）]，并根据中心线对升主动脉进行区域划分，旨在更好地认识主动脉瓣狭窄在主动脉扩张乃至成瘤中流场特征的影响。

1　材料与方法

1.1　研究对象

2017年1月至2021年12月，我们中心共招募了63名18岁以上伴有升主动脉扩张或升主动脉瘤的住院患者（最大直径≥35 mm），其中52名患者通过了质控。两位经验丰富的临床医生进行患者筛选，并采集了胸部和全主动脉CTA。本研究的实验方案及相关细节依据《赫尔辛基宣言》，并经中山大学孙逸仙纪念医院医学伦理委员会（SYSEC-KY-KS-2021-051）批准，本研究注患者知情同意。

1.1.1　CTA协议　增强CT检查涉及三种CT仪器：①美国GE公司宝石能谱CT（GE Discovery CT 750 HD）扫描，参数：管电压120 kV，管电流（270~300）mA，层厚7 mm，螺距3.0；②美国GE公司64排螺旋CT（GER evolution EVO）扫描，参数：管电压120 kV，管电流（100~350）mA，层厚5 mm，螺距1.0；③西门子64层螺旋CT（Somatom Sensation 64, Siemens, Germany）扫描。扫描范围涵盖下颌至膈肌。扫描主要参数：管电压120 kV，管电流（200~500）mA，准直64 mm×0.6 mm，螺距0.8。增强扫描主要参数及扫描范围同平扫，经肘静脉团注非离子型对比剂（碘佛醇320），剂量（1.5~2.0）mL/kg，注射流率（4~6）mL/s。自动触发扫描，触发点放置于升主动脉层面，触发阈值100 HU，采用一次屏气完整扫描，扫描方向为头至足。扫描范围视检查需求。将CT数据以DICOM（digital imaging and communications in medicine）格式存储。

1.1.2　纳入排除标准　纳入标准：同一时间完善心脏彩超、主动脉CTA，且影像结果提示主动脉瓣狭窄（瓣口面积≤1.5 cm^2）合并升主动脉扩张或升主动脉瘤的住院患者（最大直径≥35 mm）；正常主动脉瓣（瓣口面积≥1.5 cm^2）合并升主动脉扩张或升主动脉瘤住院患者。排除标准：①先天性大血管畸形、升主动脉瘤合并夹层、脉管炎、自身免疫病、感染性动脉瘤、胸部外伤史、既往心脏、大血管、纵膈手术史。②图像质量不符合后处理要求的：CTA图像质量过差、伪影严重无法完整进行仿真建模、图像残缺未涵盖完整主动脉的。

1.2　倾向评分匹配

为了避免混杂因素对研究的影响，我们使用倾向评分匹配（propensity score matching, PSM）对患

者及其临床资料进行倾向性匹配。设置卡钳值为0.1并经过1:1匹配后,十个混杂变量(年龄、性别、CT设备、吸烟史、糖尿病史、高血压史、冠心病史、心律失常史、高脂血症史和升主动脉最大内径)在两组间差异无统计学意义($P>0.1$;如表1所示)。

1.3 CFD模拟

CFD的过程包括升主动脉的分割及重建(图1A、B、C所示)、建立升主动脉网格(图1D所示)和血流动力学计算[9-11](图1E)。

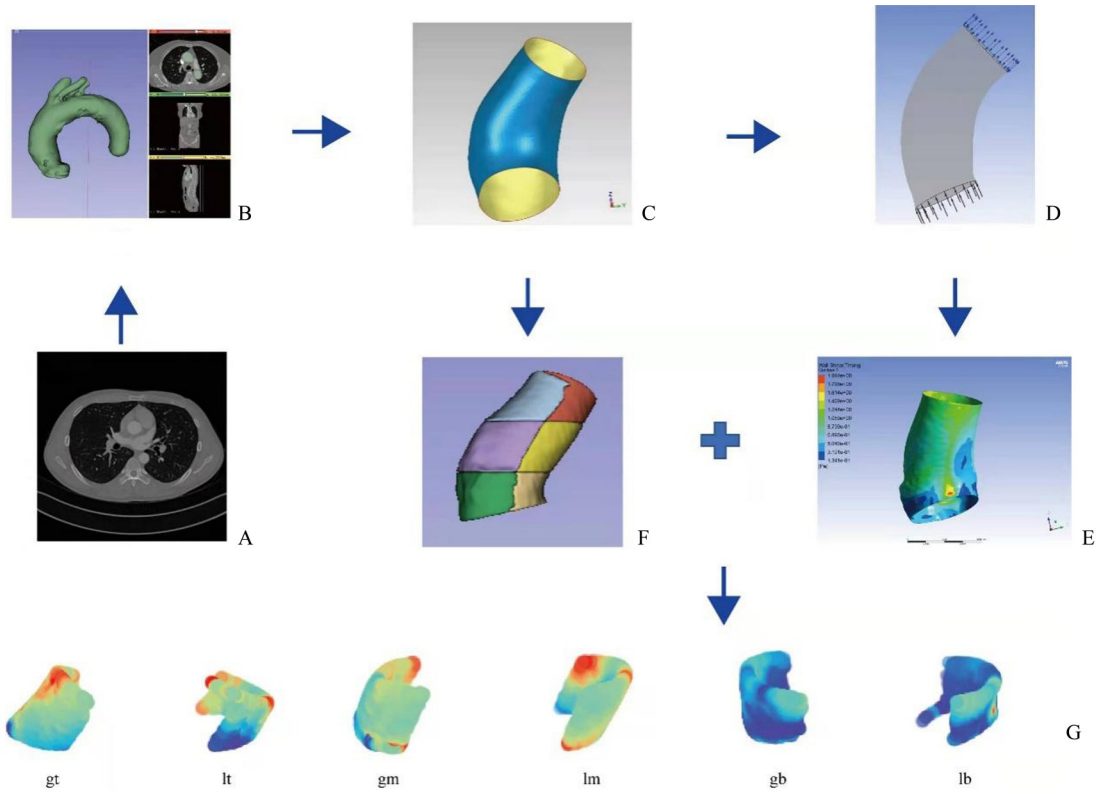

Shortly, we first labelled the mask of aorta (B) from the raw CTA (A). The ascending aorta was cropped, smooth and refine (C). Boundary conditions were set for hemodynamics calculation (D). Results, including pressure, wall shear stress and so on, were obtained after post-processing (E). Then we split ascending aorta into 6 parts (gt, gm, gb, lt, lm, lb) by the centerline (F, G). Gt: the top region of greater curvature of ascending aorta. Gm: the middle region of greater curvature of ascending aorta. Gb: the bottom region of greater curvature of ascending aorta. Lt: the top region of lesser curvature of ascending aorta. Lm: the middle region of lesser curvature of ascending aorta. Lb: the bottom region of lesser curvature of ascending aorta.

图1 CFD及升主动脉分割的流程图

Fig. 1 The architecture of CFD and the ascending aortic segmentation

1.3.1 *升主动脉的分割及重建* 使用开源软件3D Slicer(版本=4.11.01)[12]处理患者DICOM格式的CTA(图1A),标记胸主动脉使其包含主动脉根部、主动脉窦、窦管交界处(sinotubular junction, STJ)、升主动脉、弓部、降主动脉和主要分支(图1B)。经过平滑处理后,并导入Geomagic Studio 2012软件中裁剪、平滑和细化升主动脉(从STJ起到头臂干起始端止),获取升主动脉壁面片模型,并保存为立体光刻的格式(STL,图1C)。

1.3.2 *建立升主动脉网格* 使用Ansys Student 2020 R2系列软件建立升主动脉网格。固体域包括入口、出口和壁面,其中,定义入口为STJ,出口为头臂干起始端,壁面为血管壁,流体域为血流。网格包括体网格和边界层网格,其中,体网格为四面体为主的网格[13],通过前期网格独立性验证及既往研究确定网格数在1.5×10^7以上[14];边界层为6层0.01 mm厚的网格,以满足对近壁面指标如WSS的精确计算[9]。在网格生成和质量优化后,导出网格。

1.3.3 *血流动力学计算* 将网格文件导入Ansys Student CFX 2020 R2软件中,根据Navier-Stokes方程,通过结合有限元法和有限体积法进行瞬态求解(图1D)。边界条件设置如下:血管壁定义为无滑

移的刚性壁；血液性质为非牛顿流体，在体温37 ℃条件下，血液密度ρ为1 060 kg/m^3，黏度μ为0.003 5 Pa/s[11]；一个心动周期（T）为0.8 s，并均分为100个时间步，每个时间步步长为0.008 s；根据既往研究获得入口处流速-时间曲线及出口压力-时间曲线[15-17]。根据本研究边界条件设置，最大雷诺数为10 221，故采用湍流模型Re-Normalisation Group mode（RNG）k-ε进行计算[18-20]。每时间步进行30次迭代，使用均方根误差（root mean square，RMS）进行残差监测，当RMS $<1\times10^{-6}$即视为收敛，方可进入下一时间步进行计算。完成CFD计算后导入CFD-Post进行后处理，输出升主动脉壁各节点在心动周期内的峰值压力、WSS、SSR和一个心动周期内的TAWSS、TASSR（图1E）[21]。

1.4　划分升主动脉区域

根据升主动脉中心线长度及走行，将升主动脉平均分为六块具有独特空间特征的区域（大弯上段，小弯上段，大弯中段，小弯中段，大弯下段，小弯下段，如图1F、G所示）。

1.5　统计学分析

我们在统计分析中使用Python3.8版本。正态分布的连续变量用其均数±标准差表示，非正态分布的连续变量用中位数（下四分位数~上四分位数）[M（P_{25}~P_{75}）]表示，分类变量用数字（百分比）表示。符合正态分布的定量资料采用两样本t检验，不符合正态分布的定量资料采用Wilcoxon秩和检验，不符合正态分布的配对定量资料采用Wilcoxon符号秩和检验，分类资料组间比较使用卡方检验或Fisher's精确检验。P值<0.05为差异具有统计学意义。双侧检验用于比较两组患者的血流动力学指标是否有差异，单侧检验用于具体分析两组患者血流动力学指标的差异。

2　结　果

2.1　临床的基线资料

在2017年至2020年间，我们共纳入了52名18岁以上伴有升主动脉扩张或升主动脉瘤的住院患者（最大直径≥35 mm）患者，其中21（40.38 %）名患者被诊断为主动脉瓣狭窄合并升主动脉扩张，其余31（59.62 %）名升主动脉扩张患者未合并主动脉瓣狭窄。患者的平均年龄为（63.45±10.88）岁，男性人数为36（69.23 %），升主动脉的平均直径为（49.59±8.74）mm。

经过PSM匹配后，共22例患者（主动脉瓣狭窄组11例，非狭窄组11例）纳入本研究，且年龄、性别、CT设备、吸烟史、糖尿病史、高血压史、冠心病史、心律失常史、高胆固醇史、最大直径这十个变量在主动脉瓣狭窄组及非狭窄组间差异无统计学意义（$P>0.05$，如表1所示）。

2.2　CFD结果

经求解，所有22名患者各时间步CFD计算结果均达到收敛，准确获取到各患者一个心动周期内升主动脉壁各节点峰值WSS、SSR、压力和TAWSS、TASSR数值和分布。

2.2.1　不同主动脉瓣膜的升主动脉血流动力学指标之间的差异　经过统计检验，在不同主动脉瓣膜的患者血流动力学指标中，SSR和WS的差异存在统计学意义，而压力、TASSR和TAWSS的差异无统计学意义（表2）。

2.2.2　主动脉瓣狭窄患者及非狭窄患者相同升主动脉区域的血流动力学分析　既往研究多将升主动脉视为一个整体，计算血流动力学指标的中位数或均值，可根据本研究的结果可知升主动脉不同区域存在较大的差异（如图1G、图2A所示），经过上述划分方法，可以科学地将升主动脉划分为6个具有独特血管形态学特征的区域，更加合理地比较两组患者相同区域的血流动力学差异（图2）。

在主动脉瓣狭窄组及非狭窄组的患者中，升主动脉6个相同区域的压力、TASSR、TAWSS差异无统计学意义（图2B，E，F）；而SSR中，升主动脉大弯侧下段（$Z=3.021$，$P=0.003$）、小弯侧上段（$Z=1.970$，$P=0.04$）、小弯侧中段（$Z=2.430$，$P=0.02$）和小弯侧下段（$Z=3.349$，$P<0.001$）的差异存在统计学意义（图2C）；WSS中，升主动脉大弯侧下段（$Z=3.086$，$P=0.002$）、小弯侧上段（$Z=2.233$，$P=0.03$）、小弯侧中段（$Z=2.561$，$P=0.01$）和小弯侧下段（$Z=3.349$，$P<0.001$）的差异存在统计学意义（图2D）。后续单侧检验显示主动脉瓣狭窄组升主动脉下段及小弯侧的SSR和WSS高于非狭窄组（如表3所示）。

3　讨　论

本研究中，我们纳入了主动脉瓣狭窄合并升主动脉瘤患者及根据其临床基线资料进行倾向性评

表1 PSM后混杂因素构成比差异的比较

Table 1 Comparison of the constituent ratio of confounding factors after PSM

Variables	Level	AS	None	t/χ^2	P
Age/years		63.82±9.30	62.55±9.06	t = 0.312	0.768
Sex	Male	10 (91)	10 (91)		1.000
CT	Siemens Force	8 (73)	6 (54)		
	GE CT750	3 (27)	4 (36)	χ^2 = 1.429, ν= 2	0.496
	EVO	0 (0)	1 (1)		
Smoke	Yes	9 (82)	9 (82)		1.000
Diabetes	Yes	10 (91)	10 (91)		1.000
Hypertension	Yes	9 (82)	10 (91)		1.000
hypercholesteremia	Yes	10 (91)	10 (91)		1.000
CHD	Yes	4 (36)	5 (45)		1.000
Arrhythmia	Yes	10 (91)	10 (91)		1.000
Maximum diameter/mm		49.75±9.3	49.64±4.81	t = 0.034	0.973

PSM: propensity score matching; CHD: coronary heart disease; AS: aortic valve stenosis; None: normal aortic valve; normally distributed continuous variables were represented by their mean ± standard deviations, categorical data by the numbers (percentages). Pearson's chi-square test or Fisher's exact test was performed in categorical variables and t test was performed in age and maximum diameter; all tests were 2-tailed; P value < 0.05 was regarded as significant.

表2 不同主动脉瓣膜的升主动脉血流动力学指标

Table 2 Hemodynamic indexes of ascending aorta with different aortic valves

Hemodynamic indexes	AS	None	Z	P
Pressure/Pa	15 633.19 (15 230.07~15 839.88)	15 632.26 (15 568.89~15 681.29)	0.394	0.694
SSR/s	191.70 (117.22~248.78)	93.23 (68.59~145.35)	2.167	0.030
WSS/Pa	2.87 (1.88~4.00)	1.20 (1.04~2.18)	2.233	0.026
TASSR/s	57.20 (48.12~80.15)	52.12 (44.15~125.97)	0.000	1.000
TAWSS/Pa	0.70 (0.58~1.11)	0.68 (0.52~1.95)	0.000	1.000

AS: aortic valve stenosis; None: normal aortic valve; SSR: shear stress rate; WSS: wall shear stress; TASSR: time averaged shear stress rate; TAWSS: time average wall shear stress; non-normally distributed continuous variables were presented by median (interquartile range); Mann-Whitney U test was used in comparisons between groups; all tests were 2-tailed; P value < 0.05 was regarded as significant.

分匹配的无主动脉瓣狭窄的升主动脉瘤患者,通过标准化地提取CTA中的升主动脉进行仿真建模、基于有限元和有限体积法的CFD瞬态计算,发现合并主动脉瓣狭窄的升主动脉瘤患者,其升主动脉壁中位峰值WSS、SSR较不合并主动脉瓣狭窄的患者显著升高。同时,为进一步研究分布差异,我们将升主动脉均分为6份,发现在大弯近端、小弯近端、小弯中部和小弯远端侧,合并主动脉瓣狭窄的动脉瘤患者WSS、SSR水平升高。

虽然目前研究都聚焦于主动脉瓣二叶瓣畸形导致的升主动脉病[22],但目前研究发现,无论是二叶瓣还是三叶瓣导致的主动脉瓣狭窄,都将不同程

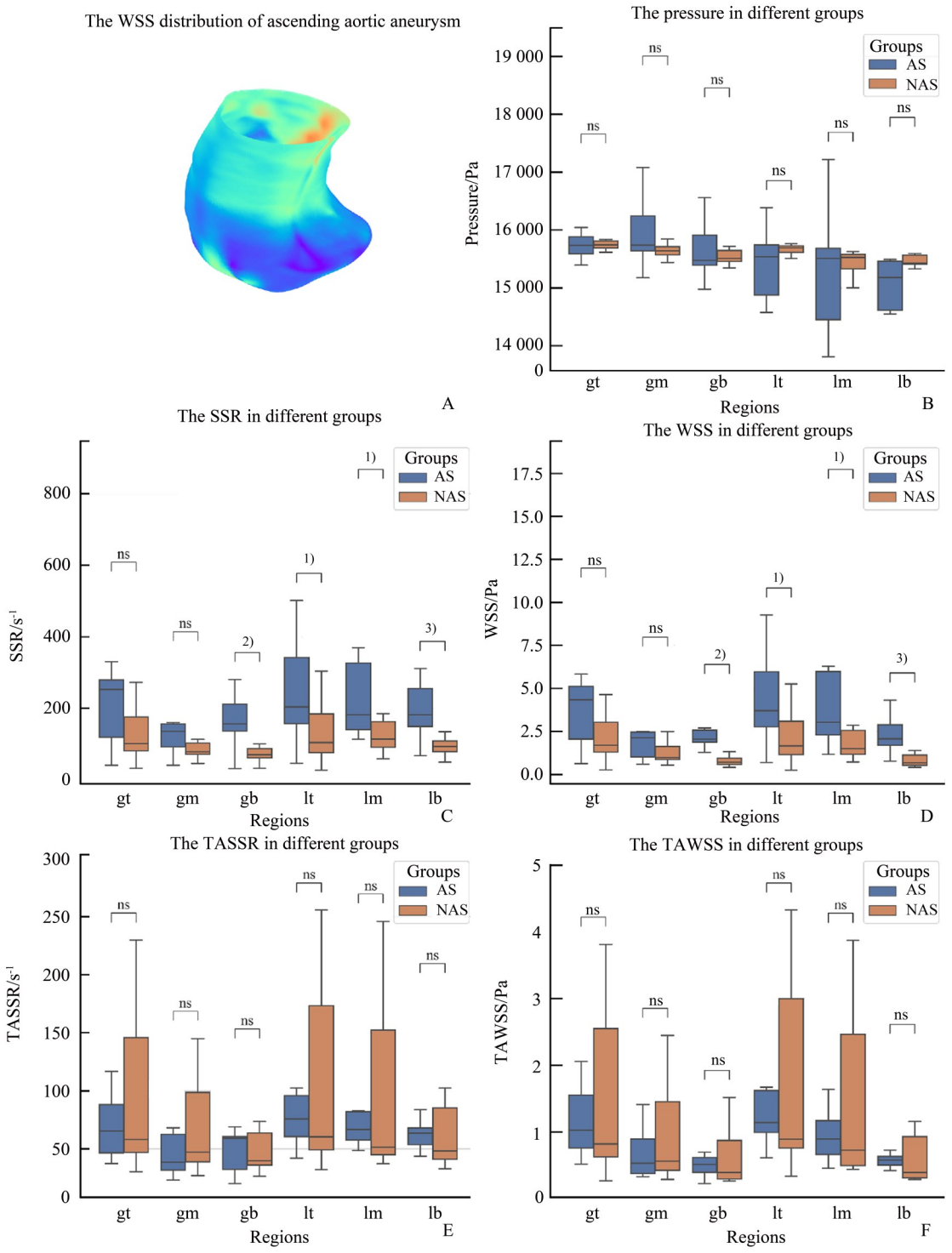

The distribution of WSS varies greatly in different regions of ascending aorta (A). Pressure (B), SSR (C), WSS (D), TASSR (E), TAWSS (F) in ascending aorta that suffered from dilation with two different kinds of aortic valves in 22 patients. Mann-Whitney *U* test was used in comparisons between groups. All tests were 2-tailed. *P* value < 0.05 was considered significant. AS: aortic valve stenosis. None: normal aortic valve. SSR: shear stress rate. WSS: wall shear stress. TASSR: time averaged shear stress rate. TAWSS: time average wall shear stress. Gt: the top region of greater curvature of ascending aorta. Gm: the middle region of greater curvature of ascending aorta. Gb: the bottom region of greater curvature of ascending aorta. Lt: the top region of lesser curvature of ascending aorta. Lm: the middle region of lesser curvature of ascending aorta. Lb: the bottom region of lesser curvature of ascending aorta. ns: There was no statistical significance. [1)] $P < 0.05$; [2)] $P < 0.01$; [3)] $P < 0.001$.

图2　升主动脉血流动力学指标

Fig. 2　Hemodynamic indexes of ascending aorta

表3 主动脉瓣狭窄改变升主动脉瘤的流场特征

Table 3 Aortic valve stenosis changed the flow field characteristics of ascending aortic aneurysm

Hemodynamic indexes	Regions	AS	None	*Z*	*P*
SSR/s	gb	156.36 (136.23~211.41)	70.00 (61.22~87.44)	3.021	0.001
	lt	203.91 (156.69~341.05)	103.89 (76.14~183.65)	1.970	0.024
	lm	181.61 (140.42~326.08)	113.26 (91.34~162.07)	2.430	0.007
	lb	181.58 (149.10~255.50)	93.02 (78.39~108.37)	3.349	< 0.001
WSS/Pa	gb	2.04 (1.88~2.57)	0.70 (0.59~0.95)	3.086	0.026
	lt	3.71 (2.75~5.96)	1.66 (1.16~3.10)	2.233	0.013
	lm	3.04 (2.31~5.99)	1.51 (1.17~2.55)	2.561	0.005
	lb	2.08 (1.70~2.89)	0.67 (0.53~1.13)	3.349	< 0.001

Gb: the bottom region of greater curvature of ascending aorta. Lt: the top region of lesser curvature of ascending aorta. Lm: the middle region of lesser curvature of ascending aorta. Lb: the bottom region of lesser curvature of ascending aorta. AS: aortic valve stenosis; None: normal aortic valve; SSR: shear stress rate; WSS: wall shear stress; non-normally distributed continuous variables were presented by median (interquartile range); Mann-Whitney *U* test was used in comparisons between groups; all tests were 1-tailed; *P* value < 0.05 was regarded as significant.

度地影响主动脉管壁,导致血管扩张程度和管壁顺应性不协调,诱发主动脉瘤和夹层[23]。且对于伴不伴随主动脉瓣病变的主动脉扩张或动脉瘤,其血流动力学特征有明显差异。一项针对571名患者的临床研究显示[24],合并主动脉瓣狭窄的升主动脉扩张的患者的WSS值较不伴有主动脉瓣狭窄的主动脉瘤患者显著升高,且4个分区内存在显著性差异。此外,也有基于CTA的研究证实,合并重度主动脉瓣狭窄的主动脉瘤患者中,WSS水平较无狭窄或轻度狭窄的患者水平升高,且这种水平升高和主动脉瓣病变导致的升主动脉几何特征改变有关[25]。本研究中我们发现,对于合并主动脉瓣狭窄的动脉瘤患者,其WSS水平相应升高及由WSS衍生的SSR亦同步升高,与前述文献结果相一致。然而,相比较于不合并主动脉瓣狭窄的升主动脉扩张患者,其TAWSS和TASSR未见统计学差异,可能是由于大动脉的弹性储器特性在心动周期内对血流的调节作用[26]。此外,相较于其他文献,我们也分析了压力分布情况,我们发现,实验组和对照组的压力水平差异[23]无统计学意义,这提示我们WSS及其衍生指标可能是主动脉瓣狭窄合并动脉扩张的显著生物力学特征,且有望成为评价主动脉瓣狭窄患者升主动脉生物力学特性的重要指标之一。

虽然多个研究揭示了不同病因的升主动脉扩张的流体力学特性,但对于其具体的分布仍研究较少,且主要在二叶瓣畸形导致的主动脉扩张方面[27]。前述Van等[24]的研究中,通过纳入大量病例,研究了主动脉瓣狭窄合并主动脉扩张的患者的WSS改变情况及其分区,虽观察指标仅有WSS,但其结论仍提示我们,在主动脉瓣狭窄合并升主动脉扩张的患者中,其流体力学指标的差异有空间特异性。因此,本研究中,我们纳入了本中心的国人数据,构建了升主动脉的6个分区,比较了各分区下压力、WSS、TAWSS、SSR、TASSR的空间分布差异。对于合并AS的升主动脉瘤患者,在升主动脉大、小弯近端和小弯侧中部、远端4个区域,WSS和SSR的数值均较不合并AS的主动脉瘤患者升高,其分布差异大致与Van等[24]的研究一致,而压力指标无

明显统计学差异，这提示了AS前向血流模式改变与AS继发的主动脉瘤血流动力学特征异常相关。上述血流动力学指标的空间分布差异改变的机制目前仍未完全阐明，可能与主动脉瓣狭窄流场模式异常及其继发的升主动脉几何特性改变有关，并可能进一步导致升主动脉瘤的进展和夹层的形成[28]。

本研究使用完全真实的主动脉瘤患者CTA数据，通过准确、标准化的仿真建模手段进行分析。有限元建模部分，我们使用四面体网格和6层0.01 mm厚的边界层网格，以准确计算包括WSS在内的近壁面参数。由于主动脉中血液的不可压缩性和主动脉壁的无滑移特性，血液的形变是可以忽略不计的，故本研究中将血液理想化为非牛顿流体进行运算[11,29]。对于出入口边界条件设置，我们根据既往文献重新拟合和简化了[15,30]主动脉瓣狭窄和无狭窄升主动脉瘤患者的速度-时间和压力-时间曲线，以在保证最大程度符合主动脉血流动力学特征的基础上提高运算效率，并避免了曲线过拟合的风险。同时，为了最大程度地模拟体内主动脉的流体力学特征，我们根据雷诺数选择了合适的湍流模型用于我们的主动脉瞬态模型计算中，以保证建模的准确性。

综上，本研究发现了在合并主动脉瓣狭窄的升主动脉瘤患者中，WSS、SSR较不合并主动脉瓣狭窄的患者有所升高。同时，这种血流动力学特征的改变具有空间特异性，即在升主动脉近端、小弯侧升高显著。相比较于压力、TAWSS等在升主动脉瘤中特征性的指标，WSS和SSR的改变在主动脉瓣狭窄合并升主动脉瘤扩张的患者中更具有特征性意义。作为主动脉瓣狭窄合并升主动脉瘤新的流体力学特征，上述流体力学指标数值和分布的特征性改变有望为深入认识主动脉瓣狭窄对升主动脉瘤形成和进展、病变严重程度和治疗方法革新提供新思路。

然而，本研究仍具有一定局限性。本研究为单中心回顾性研究，纳入病例数有限，要进一步深入研究，仍需要多中心、大样本、前瞻性数据予以进一步证实。本研究所用的流速-时间曲线和压力-时间曲线，虽来源于文献且最大程度模拟升主动脉血流动力学特点，但由于无法获取患者检查时的主动脉流速和压力等确切数据，不能完美反应单个患者个体化的升主动脉流体力学特征。

参考文献

[1] 高润霖. 中国心瓣膜病现状[J]. 华西医学, 2018, 33(2): 127-131.
Gao RL. Current status of valvular heart disease in China[J]. West Chin Med J, 2018, 33(2): 127-131.

[2] Goody PR, Hosen MR, Christmann D, et al. Aortic valve stenosis: from basic mechanisms to novel therapeutic targets [J]. Arterioscler Thromb Vasc Biol, 2020, 40: 885-900.

[3] Youssefi P, Gomez A, Arthurs C, et al. Impact of patient-specific inflow velocity profile on hemodynamics of the thoracic aorta[J]. J Biomech Eng, 2018, 140(1). doi:10.1115/1.4037857.

[4] Pasta S, Agnese V, Gallo A, et al. Shear stress and aortic strain associations with biomarkers of ascending thoracic aortic aneurysm[J]. Ann Thorac Surg, 2020, 110(5): 1595-1604.

[5] Dux-Santoy L, Guala A, Sotelo J, et al. Low and oscillatory wall shear stress is not related to aortic dilation in patients with bicuspid aortic valve: a time-resolved 3-dimensional phase-contrast magnetic resonance imaging study[J]. Arterioscler Thromb Vasc Biol, 2020, 40(1): e10-e20.

[6] Ramaekers MJFG, Adriaans BP, Juffermans JF, et al. Characterization of ascending aortic flow in patients with degenerative aneurysms: a 4D flow magnetic resonance study [J]. Invest Radiol, 2021, 56(8): 494-500.

[7] Batchelor GK. An introduction to fluid dynamics[M]. Cambridge: Cambridge University Press, 2000. doi: 10.1017/CBO9780511800955.

[8] Hoi Y, Meng H, Woodward SH, et al. Effects of arterial geometry on aneurysm growth: three-dimensional computational fluid dynamics study[J]. J Neurosurg, 2004, 101(4): 676-681.

[9] Febina J, Sikkandar MY, Sudharsan NM. Wall shear stress estimation of thoracic aortic aneurysm using computational fluid dynamics[J]. Comput Math Methods Med, 2018, 2018: 7126532.

[10] Kalykakis GE, Antonopoulos AS, Pitsargiotis T, et al. Relationship of endothelial shear stress with plaque

features with coronary CT angiography and vasodilating capability with PET[J]. Radiology, 2021, 300(3): 549-556.
[11] Midulla M, Moreno R, Baali A, et al. Haemodynamic imaging of thoracic stent-grafts by computational fluid dynamics (CFD): presentation of a patient-specific method combining magnetic resonance imaging and numerical simulations[J]. Eur Radiol, 2012, 22(10): 2094-2102.
[12] Fedorov A, Beichel R, Kalpathy-Cramer J, et al. 3D Slicer as an image computing platform for the quantitative imaging network[J]. Magn Reson Imaging, 2012, 30(9): 1323-1341.
[13] Thondapu V, Tenekecioglu E, Poon EKW, et al. Endothelial shear stress 5 years after implantation of a coronary bioresorbable scaffold[J]. Eur Heart J, 2018, 39(18): 1602-1609.
[14] Li G, Wang H, Zhang M, et al. Prediction of 3D Cardiovascular hemodynamics before and after coronary artery bypass surgery via deep learning[J]. Commun Biol, 2021, 4(1): 99.
[15] Neuhaus E, Weiss K, Bastkowski R, et al. Accelerated aortic 4D flow cardiovascular magnetic resonance using compressed sensing: applicability, validation and clinical integration[J]. J Cardiovasc Magn Reson, 2019, 21(1): 65.
[16] Stadlbauer A, van der Riet W, Crelier G, et al. Accelerated time-resolved three-dimensional MR velocity mapping of blood flow patterns in the aorta using SENSE and k-t BLAST[J]. Eur J Radiol, 2010, 75(1): e15-21.
[17] Cong M, Zhao H, Dai S, et al. Transient numerical simulation of the right coronary artery originating from the left sinus and the effect of its acute take-off angle on hemodynamics[J]. Quant Imaging Med Surg, 2021, 11(5): 2062-2075.
[18] Miyazaki S, Itatani K, Furusawa T, et al. Validation of numerical simulation methods in aortic arch using 4D flow MRI[J]. Heart Vessels, 2017, 32(8): 1032-1044.
[19] Hohri Y, Numata S, Itatani K, et al. Prediction for future occurrence of type A aortic dissection using computational fluid dynamics[J]. Eur J Cardiothorac Surg, 2021, 60(2): 384-391.
[20] Banks J, Bressloff NW. Turbulence modeling in three-dimensional stenosed arterial bifurcations[J]. J Biomech Eng, 2007, 129(1): 40-50.
[21] Erbel R, Aboyans V, Boileau C, et al. 2014 ESC Guidelines on the diagnosis and treatment of aortic diseases: Document covering acute and chronic aortic diseases of the thoracic and abdominal aorta of the adult. The Task Force for the Diagnosis and Treatment of Aortic Diseases of the European Society of Cardiology (ESC)[J]. Eur Heart J, 2014, 35(41): 2873-2926.
[22] Afzal S, Piayda K, Maier O, et al. Current and future aspects of multimodal imaging, diagnostic, and treatment strategies in bicuspid aortic valve and associated aortopathies[J]. J Clin Med, 2020, 9(3): 662.
[23] Singh A, Horsfield MA, Bekele S, et al. Aortic stiffness in aortic stenosis assessed by cardiovascular MRI: a comparison between bicuspid and tricuspid valves[J]. Eur Radio, 2019, 29(5): 2340-2349.
[24] Van Ooij P, Markl M, Collins JD, et al. Aortic valve stenosis alters expression of regional aortic wall shear stress: new insights from a 4-dimensional flow magnetic resonance imaging study of 571 subjects[J]. J Am Heart Assoc, 2017, 6(9): e005959.
[25] Doyle BJ, Norman PE, Hoskins PR, et al. Wall stress and geometry of the thoracic aorta in patients with aortic valve disease[J]. Ann Thorac Surg, 2018, 105(4): 1077-1085.
[26] Narayan O, Parker KH, Davies JE, et al. Reservoir pressure analysis of aortic blood pressure: an in-vivo study at five locations in humans[J]. J Hypertens, 2017, 35(10): 2025-2033.
[27] Guala A, Dux-Santoy L, Teixido-Tura G, et al. Wall shear stress predicts aortic dilation in patients with bicuspid aortic valve[J]. JACC Cardiovasc Imaging, 2022, 15(1): 46-56.
[28] Vergara C, Viscardi F, Antiga L, et al. Influence of bicuspid valve geometry on ascending aortic fluid dynamics: a parametric study[J]. Artif Organs, 2012, 36(4): 368-78.
[29] Perinajová R, Juffermans JF, Westenberg JJM, et al. Geometrically induced wall shear stress variability in CFD-MRI coupled simulations of blood flow in the thoracic aortas[J]. Comput Biol Med, 2021, 133: 104385.
[30] Garcia J, Barker AJ, Markl M. The role of imaging of flow patterns by 4d flow MRI in aortic stenosis[J]. JACC Cardiovasc Imaging, 2019, 12(2): 252-266.

(编辑 余 菁)